Prognostic and Predictive Values of MAD2L1 in Cholangiocarcinoma

Yuan Gao
Changzhou No.2 People's Hospital https://orcid.org/0000-0002-2140-0092
Xiwu Ouyang
Central South University First Hospital: Xiangya Hospital Central South University
Tianping Luo
Nanjing Medical University
Chunfu Zhu
Nanjing Medical University
Xihu Qin (qinxihu@126.com)
Changzhou No.2 People's Hospital

Research

Keywords: cholangiocarcinoma, bioinformatics, MAD2L1, biomarker

Posted Date: September 18th, 2020

DOI: https://doi.org/10.21203/rs.3.rs-74142/v1

Abstract

Background: This study aimed to investigate the expression of Mitotic arrest deficient 2-like protein 1 (MAD2L1) in cholangiocarcinoma (CCA) and its biological function.

Methods: Our study performed bioinformatics to analyze the microarray data from the Gene Expression Omnibus (GEO) database and obtained the differentially expressed genes (DEGs). Enrichment assay and protein-protein interaction networks analysis were conducted to extract hub genes. Mitotic arrest deficient 2-like protein 1 (MAD2L1) was investigated in tumor and adjacent nonneoplastic biliary ducts in 42 samples by immunohistochemistry. Subsequently, MAD2L1 was manipulated, and its function was examined in CCA cell lines and *in vivo* model.

Results: 297 DEGs were extracted from the microarray data. And seven hub genes were defined through the enrichment assay and protein-protein interaction networks analysis. MAD2L1 was picked up as a novel biomarker, according to hierarchical cluster analysis and Kaplan-Meier survival analysis. MAD2L1 was specifically expressed in cancer tissues but not in the surrounding normal tissue, and 31 (73.81%) of 42 CCAs were MAD2L1 positive by immunohistochemistry. MAD2L1 expression was significantly correlated with tumor size, pathological grade, and clinical stage. Kaplan-Meier analysis demonstrated an inverse correlation between MAD2L1 expression and overall survival. Real-time polymerase chain reaction (RT-PCR) and Immunoblotting results further confirmed the results of immunohistochemistry and bioinformatic analysis from the database. In *vitro* and in *vivo* models, decreasing MAD2L1 could significantly suppress tumor growth.

Conclusion: High MAD2L1 expression predicts the advanced stage of CCA. Targeting MAD2L1 may be a potential tumor suppressor and may provide the biological basis for a new therapeutic strategy.

Trial registration: [2020]KY157-01. Registered 1st April 2020 - Retrospectively registered, http://114.255.48.20/login#.

Background

Cholangiocarcinoma (CCA) is the second most prevalent liver cancer and accounts for approximately 15% of all liver cancer in adults [1]. Depending on the anatomical location of tumor initiation, CCAs are classically subtyped into three groups: intrahepatic CCA (iCCA), perihilar CCA (pCCA), and distal CCA (dCCA) [2]. But the common pathological characteristic of these three CCAs is initiating from the malignant bile duct epithelial cells [3]. Because of the improvement in the diagnosis of CCA, incidence, and mortality are both increasing all over the world, especially the east Asian [4–7]. Unfortunately, to date, there has been still no satisficing therapeutic strategy except for surgical resection and liver transplant [7, 8]. Data from the past 30 years suggests that the 5-year overall survival rate has shown no improvement [9]. The dominating reasons are approximately 65% of patients are diagnosed with unresectable, and over 90% of patients recurrent early after surgical treatment [10, 11]. Developing novel biomarkers for

improving early diagnosis, monitoring recurrence, and exploring new mechanisms underlying CCA progression is urgent.

In the past two decades, microarray technology and bioinformation have been widely applied to analyze the gene expression in CCA [12, 13]. More and more microarray data has been uploaded to the Gene Expression Omnibus (GEO) database for sharing. Screening genetic alterations from GEO and identifying the differentially expressed genes (DEGs) and pathways involved in carcinogenesis is an emerging strategy for cancer research [14, 15].

In our study, we searched from GEO and got three mRNA microarray datasets. After standardization, we analyzed to obtain DEGs between carcinoma tissues and non-carcinoma tissues. Whereafter, online bioinformatics analysis including Gene Ontology (GO), Kyoto Encyclopedia of Genes and Genomes (KEGG) pathway enrichment analysis, and protein-protein interaction (PPI) network were performed to explore the molecular mechanisms underlying tumorigenesis and progression. MAD2L1, one of the DEGs, was validated high expression in tumors and correlated with poor survival in CCA from the TCGA database. Then, we investigated the expression of MAD2L1 in tumor tissues, adjacent nonneoplastic biliary duct from CCA patients by immunohistochemistry (IHC) in 42 surgically resected primary CCAs from a single institute. We also investigated the correlation of MAD2L1 expression with histologic tumor grade, progression, metastasis, clinical stage, and postoperative survival rate. Functional exploration, we altered MAD2L1 in CCA cell lines and assayed cell proliferation, and results demonstrated that MAD2L2 could promote cell growth. And the *in vivo* study results also confirmed the *in vitro* study. In conclusion, we found MAD2L1 could be a novel biomarker in CCA, and targeting MAD2L1 may be a potential therapeutic strategy for CCA.

Methods

Microarray data. Three gene expression datasets [GSE26566, GSE32225, and GSE77984] were downloaded from GEO. The GSE26566 dataset contained 104 human cholangiocarcinoma tissues and six noncancerous samples [16]. GSE32225 contained 150 tumor samples and five normal human cholangiocytes [17]. GSE77984 contained ten cholangiocarcinoma cells and 12 normal human cholangiocytes [18]. The DEGs between CCA and noncancerous samples were analyzed using GEO2R (http://www.ncbi.nlm.nih.gov/geo/geo2r). Adj.P-value <0.01, and logFC (fold change) >1 were considered statistically significant.

Bioinformatic analysis. The Database for Annotation, Visualization, and Integrated Discovery (DAVID; http://david.ncifcrf.gov) (version 6.7) was used to conduct biological analyses [19]. P<0.05 was considered statistically significant. Search Tool for the Retrieval of Interacting Genes (STRING; http://string-db.org) (version 11.0) was performed to predict the functional interactions between proteins and with a combined score >0.4 was considered statistically significant [20]. The plug-in Molecular Complex Detection (MCODE) (version 1.4.2) of Cytoscape was used to find densely connected regions with the criteria for selection as following: MCODE scores >5, degree cut-off=2, node score cut-off=0.2,

Max depth=100 and k-score=2, and the hub genes were selected with degrees ≥15 [21]. Hierarchical clustering and the overall survival analyses of hub genes were constructed using the UCSC Cancer Genomics Browser (https:// genome-cancer.ucsc.edu) [22].

Patient selection. Forty-two surgically resected primary CCAs were collected from 2004 to 2014 at our institute. The study was approved by the ethics committee and conducted following the regulations. All patients signed informed consent for the use of their CCA samples and clinical information. This study was also performed according to the ethical guidelines of the Declaration of Helsinki 2008 [23]. The specimens were anonymized and analyzed in a blinded fashion. Follow-up time for survivors ranged from 1 to 36 months (median, 15.3 months). All 42 patients were followed up for at least one year after surgery.

Histology and Immunohistochemistry. Formalin-fixed and paraffin-embedded tissue slides (5 μm) were deparaffinized and rehydrated. Antigen retrieval was performed by incubating the tissue slides in 0.01 M citric acid buffer at 100°C for 10 minutes. After blocking with 3% H_2O_2 and 5% fetal bovine serum, the slides were incubated with a monoclonal antibody against MAD2L1 (1:100, ab10691; Abcam, Burlingame, CA) at 4°C overnight. The slides were then reacted with polymer–horseradish peroxidase reagent. The peroxidase activity was visualized with diaminobenzidine tetrahydroxychloride solution. The sections were counterstained with hematoxylin. Dark brown cytoplasmic staining of at least 1% tumor cells was defined as positive, and no staining or less than 1% cells stained was defined as negative. As a negative control, we replaced the primary antibody with 5% fetal bovine serum.

Cell culture. All CCA cell lines, QBC939 was donated by Dr. Li lab [24], HuCCT1 cells were purchased from the Japanese Collection of Research Bioresources Cell Bank, and HEK293T cell lines were obtained from the American Type Culture Collection. Cells were maintained in Dulbecco's modified Eagle's medium (Invitrogen; Thermo Fisher Scientific Inc.) supplemented with 10% fetal bovine serum (Thermo Fisher Scientific, Inc.), 1% glutamine, and 1% penicillin/streptomycin (Invitrogen; Thermo Fisher Scientific, Inc.). Cells were humidified in a 5% (v/v) CO_2 environment at 37˚C. Tests for mycoplasma contamination yielded negative results by direct PCR.

Cell count. Trypan blue dye exclusion test by staining cells with 0.2% Trypan blue solution (Sigma-Aldrich Chemical Co, MO, USA) was performed to reveal necrotic cells after each experimental condition, according to the manufacturer's instructions. Moreover, unstained viable cells were manually counted using a hemocytometer. Counts were performed by triplicate under a 10X objective according to standard methodology. All measurements were performed in triplicate.

Animal experiments. Eight 6-week-old nude mice were purchased from the National cancer institute (NCI) and divided into two groups for injection of QBC939 cells transfected/engineered with (1) shNC, (2) shMAD2L1. The prepared stable QBC939 cells (mixed with Matrigel, 1:1) were injected at 1×10^6 into the Subcutaneous tissue of the mice. The mice were sacrificed after 8 weeks. Tumors were removed for study. Animal protocols were approved by the Animal Care and Use Committee of Nanjing medical

university. And all animal experiments followed guidelines for ethical review of laboratory animal welfare of Nanjing medical university (http://iacuc.njmu.edu.cn).

Lentiviral expression plasmids and virus infection. The lentivirus system with the standard calcium chloride transfection method was applied to generate the virus. pWPI vectors over-expressing MAD2L1 and pLKO.1 vectors expressing short hairpin RNA (shRNA) were used to generate lentivirus to infect CCA cells, respectively. The pWPI/pWPI-MAD2L1/pLKO.1/pLKO.1-shMAD2L1#1/pLKO.1-shMAD2L1#2 plasmids (MilliporeSigma, MA, US), pMD2G addgene,#12259envelope plasmid, and psPAX2 (addgene, #12260) packaging plasmid were co-transfected into the HEK293T cells. After 8 h, the medium was changed with a warm, fresh medium. The 293 cells (Human Embryonic Kidney 293 cells) were then placed in the virus room incubator for the generation of the virus. After 48 h, the supernatants, including the viruses, were harvested and used immediately or frozen at -80˚C for later use. The The sequences were as follows: shMAD2L1#1 targeting sequence, 5'- CCTATTGAATCAGTTTCCAAT-3'; and shMAD2L1#2 targeting sequence, 5'- CGAGTTCTTCTCATTCGGCAT-3'.

Western Bolt. Freshly frozen tissues were isolated and lysed in RIPA buffer, and proteins (30-50 μg) were separated on 6–10% SDS/PAGE gel and then transferred onto PVDF membranes (Millipore, Billerica, MA). After blocking with 5% BSA, the PVDF membranes were incubated with primary antibodies and then HRP-conjugated secondary antibodies. Subsequently, The ECL system (Thermo Fisher Scientific, Rochester, NY) was used to visualize. The primary antibodies used for western blot were, MAD2L1 (1:1000; Abcam), GAPDH (1:5000; Santa Cruz Biotechnology, Santa Cruz, CA).

Real-time polymerase chain reaction (PCR). Fresh samples were used to analyze the mRNA level of MAD2L1 by real-time polymerase chain reaction (PCR) performed with the ABI StepOnePlus PCR System (Applied Biosystems, Foster City, CA). Total RNA was extracted using TRIZOL reagent, and all primers were purchased from Invitrogen (Invitrogen, Carlsbad, CA). MAD2L1 mRNA was normalized with the GAPDH mRNA level, and results were presented as the ratio of MAD2L1 to GAPDH. The primers were as follows: MAD2L1 forward primer, 5'- ACGGTGACATTTCTGCCACT-3'; MAD2L1 reverse primer, 5'-TGGTCCCGACTCTTCCCATT-3'; GAPDH forward primer, 5'-GGAGCGAGATCCCTCCAAAAT-3', GAPDH reverse primer, 5'-GGCTGTTGTCATACTTCTCATGG-3'.

Statistics. Statistical analysis was performed using SPSS software, version 23.0 (IBM Inc.). Mann-Whitney U test was applied to test the two groups of continuous data. Correlation between MAD2L1 expression and clinicopathological parameters was evaluated by the $\chi 2$ test and Fisher exact test. Survival rates were calculated using the unadjusted Kaplan-Meier method, and the log-rank analysis analyzed the difference in survival curves. All cell experiments were conducted in three technical replicates. Quantitation results are shown as mean ± SD. Statistical significance for cell experiments was determined using the independent-sample t-test. $P<0.05$ was considered to indicate a statistically significant difference.

Results

Expression profiles and integrated screening of DEGs in human CCA tissues from bioinformatic analysis

Three microarray datasets containing cancerous and noncancerous tissues from GEO were analyzed to obtain DEGs. We firstly standardized the microarray results, then identified all DEGs (4,702 in GSE26566, 1,092 in GSE32225, and 2447 in GSE77984); lastly, overlapped the three datasets and got 297 genes as shown in the Venn diagram (**Fig. 1A**). Functional and pathway enrichment analyses of 297 DEGs were performed using DAVID, and the top 20 GO pathways were showed in **figure 1B**. The results of GO analysis demonstrated that changes in biological processes (BP) of DEGs were significantly enriched in protein binding, negative regulation of the apoptotic process. Changes in molecular function (MF) of DEGs were mainly enriched in protein binding, poly(A) RNA binding, and protein homodimerization activity. Changes in cell component (CC) of DEGs were mainly enriched in the cytoplasm, nucleus, and perinuclear region of cytoplasm (**Fig. 1B**). KEGG pathway analysis revealed that the 297 DEGs were mainly enriched in pathways in cancer (**Fig. 1C**). To further extract the hub genes from the DEGs, STRING and Cytoscape were used to predict the PPI network and get the most significant modules (**Fig. 1D**). A total of 7 genes were identified as hub genes with degrees ≥15. Hierarchical clustering showed that the hub genes could differentiate the cholangiocarcinoma samples from the noncancerous samples (**Fig. 1E**). Subsequently, the Kaplan-Meier survival analysis was performed to demonstrate the overall survival of the hub genes. MAD2L1 revealed a survival difference between high expression and low expression significantly **(Fig. 1F)**. However, no difference in overall survival was shown among the other six hub genes (**Fig. S1**).

Together, the results from **Fig. 1A-F** suggest that MAD2L1 could play important roles in the carcinogenesis or progression of CCA.

Clinical data revealed MAD2L1 expression correlated with poor outcome in CCA

To evaluate MAD2L1 expression in CCA, we applied IHC to detect MAD2L1 in 42 CCA cases. Thirty-one (73.81%) of 42 cases were MAD2L1 positive, whereas 11(26.19%) were negative. All the par-carcinoma tissues were negative, compared with tumor tissue, and intriguingly, for 30 cases (71.43%) with lymphovascular invasion, only 8(26.67%) of them had MAD2L1 expression in the metastatic lymph nodes. Representative positive staining versus negative of MAD2L1 in CCA tissue was shown in **Fig. 2A**. Next, we analyzed the correlation between MAD2L1 expression and a variety of clinicopathological features. Interestingly, MAD2L1 expression was more frequently associated with larger tumor size (OR,6.231; P=0.023), higher pathological grade (OR,5.6; P=0.048), and higher stage (OR,6.000; P=0.035). However, there was no association between MAD2L1 and metastasis (p=1.000) (**table 1**). In 42 patients with at least 12 months of follow-up, Kaplan-Meier analysis showed that patients with MAD2L1 positivity had a shorter overall postoperative survival time than did MAD2L1-negative cases (**Fig 2.B**; P=0.031). To confirm the expression of MAD2L1 in CCAs, we isolated fresh tumors, adjacent nonneoplastic biliary duct from 20 CCA cases and applied real-time PCR and immunoblot to detect MAD2L1 mRNA and protein expression. As shown in **Fig. 2C** and **D**, higher MAD2L1 mRNA was detected in larger tumors than that in

small tumors. Compared with the para-carcinoma tissues, MAD2L1 protein was exclusively detected in tumors.

Taken together, **Fig.2A-D** indicated that MAD2L1 expression could be used as a biomarker to predict prognosis in CCA.

Preclinical study using in *vitro* and *invivo* models to test the role of MAD2L1 in CCA

Previous clinical data showed that positive MAD2L1 exhibited a significant difference with tumor size but not with metastasis (**table 1**). To further validate the MAD2L1 roles in the CCA progression, we conducted the gain or loss of MAD2L1 function assay through the lentiviral system in CCA cells. MAD2L1 was knocked down in QBC939 cells with MAD2L1-shRNA (**Fig. 3A**) and over-expressed in HuCCT1 cells with MAD2L1-cDNA (**Fig. 3B**). After altering MAD2L1 in QBC939 and HuCCT1 cell lines, cell count and colony formation assay were conducted to check cell growth. The results revealed that knocking down MAD2L1 with shMAD2L1 significantly suppresses cell proliferation (**Fig. 3C**). Consistently, in HuCCT1 cells, overexpression of MAD2L1 increased cell growth (**Fig. 3D**). We performed subcutaneous tumor formation in a total of 2 groups ((1: QBC939-shNC; 2: QBC939-shMAD2L1; four nude mice for each group) as an In vivo model.. Four weeks later, the tumor volume of the shMAD2L1 group significantly reduced than the control group (**Fig. 3G and H**) due to low MAD2L1 protein level **(Fig. 3I)**

In summary, the results from **Fig. 3A-I** suggest that MAD2L1 may promote tumor progression by increasing cell proliferation.

Discussion

In our study, we applied bioinformatic analysis to find hub genes that were aberrant expression between CCA tissues and para-carcinoma tissues from GEO datasets. Firstly, we obtained 294 DEGs and employed DAVID to conduct the GO and KEGG analyses. GO enrichments demonstrated these DEGs enriched in protein binding, cytoplasm, and signal transduction, while the results of KEGG analysis revealed that DEGs enriched in pathways in cancer. Set with degrees ≥ 15, we obtained seven hub genes. Among these hub genes, Enhancer of zeste homolog 2 (EZH2) has been reported that its abnormal expression correlated with tumorigenesis and progression in many malignancies, such as cholangiocarcinogenesis, prostate cancer, and non–small cell lung carcinoma [25–27]. As a lysine methyltransferase, EZH2 catalyzes methylation of histone H3 at lysine 27, establishes and maintains H3K27 tri-methylation repressive marks [28, 29]. In physiological conditions, EZH2 plays an important role in cellular differentiation; however, in pathological conditions, it contributes to cancer cell proliferation [30]. Mechanism study in hepatocellular carcinoma (HCC) revealed that EZH2 suppressed miR-30d which could degrade Karyopherin Subunit Beta 1 (KPNB1) mRNA, and eventually increased KPNB1 expression. Ectopic expression of KPNB1 promoted HCC cell growth [31]. In the present study, EZH2 also displayed higher expression in tumor tissues compared with adjacent tissues; however, the overall survival assay showed no difference between positive and negative-EZH2. A bioinformatic study on HCC disclosed overexpression of The cell-division cycle protein 20 (CDC20), MAD2L1, and DNA replication licensing

factor (MCM3) could predict poor prognosis [32, 33]. In our study, partially due to limited clinical samples, CDC20 and MCM3 showed no difference in overall survival analysis. According to previous published functional study, these 7 hub genes correlated with the cell-division cycle in carcinoma and could be involved in cell growth [31, 34, 35].

TCGA database suggests that even all the seven hub genes displayed high expression in tumor tissues, only MAD2L1 showed a significant difference in over survival (Fig. 1F). Our clinical data confirmed that positive MAD2L1 correlated with poor survival in CCA. Positive MAD2L1 related to bigger tumor size, higher stage, and higher grade, but intriguingly no correlation was displayed between metastasis and MAD2L1-positive (**Table 1**). The IHC results of weak positive MAD2L1 in the metastatic lymph nodes backed up that MAD2L1 occupied demanding positive function in promoting tumor cell growth. To test our hypothesis, we artificially altered MAD2L1 expression in CCA cell lines and examined cell growth. The results of cell proliferation demonstrated that MAD2L1 promoted CCA cell growth. Oppositely, knocking down MAD2L1 could suppress cell growth. Previously, abundant studies illustrated that MAD2L1 plays very important roles, either in physical or pathological conditions. Physiologically, MAD2L1 exhibits synergistic action with SCF plus GM-CSF to promote the immature hematopoietic progenitor cells growth [36]. Under the pathological conditions, many upstream genes or miRNA functioned through MAD2L1 to promote cell proliferation, such as down-regulation of miR-200c-5p increased MAD2L1 expression in HCC and elevated cell growth [37, 38]. However, to date, no data showed that MAD2L1 expression in CCA. Our study has been the first study on MAD2L1 in CCA on the level of not only *vitro* but also *vivo* models. Our data demonstrated that targeting MAD2L1 could significantly suppress CCA growth, and MAD2L1 may bee a valid therapeutic target for developing more effective novel therapeutic strategies to treat CCA.

Conclusion

MAD2L1 is an oncogene. Although its function is not fully understood, the present study showed that MAD2L1 is highly expressed in cancer cells which can increase cell proliferation. MAD2L1 may be involved in multiple signaling pathways in cancer development. Therefore, the application of manipulating MAD2L1 in CCA therapy may have potential breakthroughs and become a new therapeutic target worthy of further study.

Abbreviations

MAD2L1
Mitotic arrest deficient 2-like protein 1; CCA:Cholangiocarcinoma; GEO:Gene Expression Omnibus; EZH2:Enhancer of zeste homolog 2; KPNB1:Karyopherin Subunit Beta 1;

Declarations

Ethics approval and consent to participate

This study was approved by the Clinical Research Ethics Committee of the Affiliated Changzhou No. 2 People's Hospital of Nanjing Medical University, and written informed consent was obtained from all individual participants included in the study. Clinical trial registration number is [2020]KY157-01.

Consent for publication

All included patients provided informed consent.

Availability of data and materials

All data generated or analyzed during this study are included in this published article.

Competing interests

The authors declare that they have no competing interests.

Funding

This work was partially supported by the endowment from the division of General surgery of Changzhou No. 2 People's Hospital and the Social Development Foundation of Science and Technology of Jiangsu (Grant Number: BE2016658 to XQ).

Authors' contributions

YG and XQ conceived and designed the study. LF TL XO and CZ made substantial contributions to the design of the current study, acquisition of data, interpretation of data and revising the manuscript. All authors read and approved the final manuscript.

Acknowledgements

Not applicable

References

1. Khan SA, Tavolari S, Brandi G: **Cholangiocarcinoma: Epidemiology and risk factors.** *Liver International* 2019, **39:**19-31.
2. Khan SA, Thomas HC, Davidson BR, Taylor-Robinson SD: **Cholangiocarcinoma.** *The Lancet* 2005, **366:**1303-1314.
3. Charbel H, Al-Kawas FH: **Cholangiocarcinoma: epidemiology, risk factors, pathogenesis, and diagnosis.** *Curr Gastroenterol Rep* 2011, **13:**182-187.
4. Cardinale V, Semeraro R, Torrice A, Gatto M, Napoli C, Bragazzi MC, Gentile R, Alvaro D: **Intra-hepatic and extra-hepatic cholangiocarcinoma: New insight into epidemiology and risk factors.** *World J Gastrointest Oncol* 2010, **2:**407-416.

5. Bertuccio P, Malvezzi M, Carioli G, Hashim D, Boffetta P, El-Serag HB, La Vecchia C, Negri E: **Global trends in mortality from intrahepatic and extrahepatic cholangiocarcinoma.***J Hepatol* 2019, **71:**104-114.
6. Albert JG, Waidmann O, Welzel TM: **[New insights into epidemiology may promote screening in Cholangiocarcinoma].***Dtsch Med Wochenschr* 2015, **140:**1431-1434.
7. Mukkamalla SKR, Naseri HM, Kim BM, Katz SC, Armenio VA: **Trends in incidence and factors affecting survival of patients with cholangiocarcinoma in the United States.***Journal of the National Comprehensive Cancer Network* 2018, **16:**370-376.
8. Neumann UP, Schmeding M: **Role of surgery in cholangiocarcinoma: From resection to transplantation.***Best Pract Res Clin Gastroenterol* 2015, **29:**295-308.
9. Bergquist A, von Seth E: **Epidemiology of cholangiocarcinoma.***Best Pract Res Clin Gastroenterol* 2015, **29:**221-232.
10. Rizvi S, Gores GJ: **Pathogenesis, diagnosis, and management of cholangiocarcinoma.***Gastroenterology* 2013, **145:**1215-1229.
11. Tariq NU, McNamara MG, Valle JW: **Biliary tract cancers: current knowledge, clinical candidates and future challenges.***Cancer Manag Res* 2019, **11:**2623-2642.
12. Cheng C, Hua J, Tan J, Qian W, Zhang L, Hou X: **Identification of differentially expressed genes, associated functional terms pathways, and candidate diagnostic biomarkers in inflammatory bowel diseases by bioinformatics analysis.***Experimental and Therapeutic Medicine* 2019, **18:**278-288.
13. Qian F, Guo J, Jiang Z, Shen B: **Translational Bioinformatics for Cholangiocarcinoma: Opportunities and Challenges.***International journal of biological sciences* 2018, **14:**920.
14. Liang B, Li C, Zhao J: **Identification of key pathways and genes in colorectal cancer using bioinformatics analysis.***Medical Oncology* 2016, **33:**111.
15. Yang X, Zhu S, Li L, Zhang L, Xian S, Wang Y, Cheng Y: **Identification of differentially expressed genes and signaling pathways in ovarian cancer by integrated bioinformatics analysis.***OncoTargets and therapy* 2018, **11:**1457.
16. Andersen JB, Spee B, Blechacz BR, Avital I, Komuta M, Barbour A, Conner EA, Gillen MC, Roskams T, Roberts LR, et al: **Genomic and genetic characterization of cholangiocarcinoma identifies therapeutic targets for tyrosine kinase inhibitors.***Gastroenterology* 2012, **142:**1021-1031 e1015.
17. Sia D, Hoshida Y, Villanueva A, Roayaie S, Ferrer J, Tabak B, Peix J, Sole M, Tovar V, Alsinet C, et al: **Integrative molecular analysis of intrahepatic cholangiocarcinoma reveals 2 classes that have different outcomes.***Gastroenterology* 2013, **144:**829-840.
18. Merino-Azpitarte M, Lozano E, Perugorria MJ, Esparza-Baquer A, Erice O, Santos-Laso A, O'Rourke CJ, Andersen JB, Jimenez-Aguero R, Lacasta A, et al: **SOX17 regulates cholangiocyte differentiation and acts as a tumor suppressor in cholangiocarcinoma.***J Hepatol* 2017, **67:**72-83.
19. Huang DW, Sherman BT, Tan Q, Collins JR, Alvord WG, Roayaei J, Stephens R, Baseler MW, Lane HC, Lempicki RA: **The DAVID Gene Functional Classification Tool: a novel biological module-centric algorithm to functionally analyze large gene lists.***Genome Biol* 2007, **8:**R183.

20. Franceschini A, Szklarczyk D, Frankild S, Kuhn M, Simonovic M, Roth A, Lin J, Minguez P, Bork P, von Mering C, Jensen LJ: **STRING v9.1: protein-protein interaction networks, with increased coverage and integration.***Nucleic Acids Res* 2013, **41:**D808-815.
21. Kutmon M, Ehrhart F, Willighagen EL, Evelo CT, Coort SL: **CyTargetLinker app update: A flexible solution for network extension in Cytoscape.***F1000Res* 2018, **7**.
22. Kent WJ, Sugnet CW, Furey TS, Roskin KM, Pringle TH, Zahler AM, Haussler D: **The human genome browser at UCSC.***Genome research* 2002, **12:**996-1006.
23. Williams JR: **The Declaration of Helsinki and public health.***Bull World Health Organ* 2008, **86:**650-652.
24. Wang Y, Jiang W, Li C, Xiong X, Guo H, Tian Q, Li X: **Autophagy Suppression Accelerates Apoptosis Induced by Norcantharidin in Cholangiocarcinoma.***Pathol Oncol Res* 2019.
25. Behrens C, Solis LM, Lin H, Yuan P, Tang X, Kadara H, Riquelme E, Galindo H, Moran CA, Kalhor N: **EZH2 protein expression associates with the early pathogenesis, tumor progression, and prognosis of non–small cell lung carcinoma.***Clinical cancer research* 2013, **19:**6556-6565.
26. Ren G, Baritaki S, Marathe H, Feng J, Park S, Beach S, Bazeley PS, Beshir AB, Fenteany G, Mehra R: **Polycomb protein EZH2 regulates tumor invasion via the transcriptional repression of the metastasis suppressor RKIP in breast and prostate cancer.***Cancer research* 2012, **72:**3091-3104.
27. Sasaki M, Yamaguchi J, Itatsu K, Ikeda H, Nakanuma Y: **Over-expression of polycomb group protein EZH2 relates to decreased expression of p16INK4a in cholangiocarcinogenesis in hepatolithiasis.***The Journal of Pathology: A Journal of the Pathological Society of Great Britain and Ireland* 2008, **215:**175-183.
28. Shen X, Liu Y, Hsu Y-J, Fujiwara Y, Kim J, Mao X, Yuan G-C, Orkin SH: **EZH1 mediates methylation on histone H3 lysine 27 and complements EZH2 in maintaining stem cell identity and executing pluripotency.***Molecular cell* 2008, **32:**491-502.
29. Sneeringer CJ, Scott MP, Kuntz KW, Knutson SK, Pollock RM, Richon VM, Copeland RA: **Coordinated activities of wild-type plus mutant EZH2 drive tumor-associated hypertrimethylation of lysine 27 on histone H3 (H3K27) in human B-cell lymphomas.***Proceedings of the National Academy of Sciences* 2010, **107:**20980-20985.
30. Sarma K, Margueron R, Ivanov A, Pirrotta V, Reinberg D: **Ezh2 requires PHF1 to efficiently catalyze H3 lysine 27 trimethylation in vivo.***Molecular and cellular biology* 2008, **28:**2718-2731.
31. Zhang P, Garnett J, Creighton CJ, Al Sannaa GA, Igram DR, Lazar A, Liu X, Liu C, Pollock RE: **EZH2–miR-30d–KPNB1 pathway regulates malignant peripheral nerve sheath tumour cell survival and tumourigenesis.***The Journal of pathology* 2014, **232:**308-318.
32. Zhuang L, Yang Z, Meng Z: **Upregulation of BUB1B, CCNB1, CDC7, CDC20, and MCM3 in tumor tissues predicted worse overall survival and disease-free survival in hepatocellular carcinoma patients.***BioMed research international* 2018, **2018**.
33. Yang W-X, Pan Y-Y, You C-G: **CDK1, CCNB1, CDC20, BUB1, MAD2L1, MCM3, BUB1B, MCM2, and RFC4 May Be Potential Therapeutic Targets for Hepatocellular Carcinoma Using Integrated Bioinformatic**

Analysis.*BioMed research international* 2019, **2019**.

34. Park SH, Jeong S, Kim BR, Jeong YA, Kim JL, Na YJ, Jo MJ, Yun HK, Kim DY, Kim BG: **Activating CCT2 triggers Gli-1 activation during hypoxic condition in colorectal cancer.***Oncogene* 2019**:**1-15.
35. Wei P-L, Huang C-Y, Tai C-J, Batzorig U, Cheng W-L, Hunag M-T, Chang Y-J: **Glucose-regulated protein 94 mediates metastasis by CCT8 and the JNK pathway in hepatocellular carcinoma.***Tumor Biology* 2016, **37:**8219-8227.
36. Ito S, Mantel CR, Han M-K, Basu S, Fukuda S, Cooper S, Broxmeyer HE: **Mad2 is required for optimal hematopoiesis: Mad2 associates with c-Kit in MO7e cells.***Blood* 2006, **109:**1923-1930.
37. Li Y, Bai W, Zhang J: **MiR-200c-5p suppresses proliferation and metastasis of human hepatocellular carcinoma (HCC) via suppressing MAD2L1.***Biomedicine & Pharmacotherapy* 2017, **92:**1038-1044.
38. Shi Y-X, Zhu T, Zou T, Zhuo W, Chen Y-X, Huang M-S, Zheng W, Wang C-J, Li X, Mao X-Y: **Prognostic and predictive values of CDK1 and MAD2L1 in lung adenocarcinoma.***Oncotarget* 2016, **7:**85235.

Tables

Due to technical limitations, table 1 is only available as a download in the Supplemental Files section.

Figures

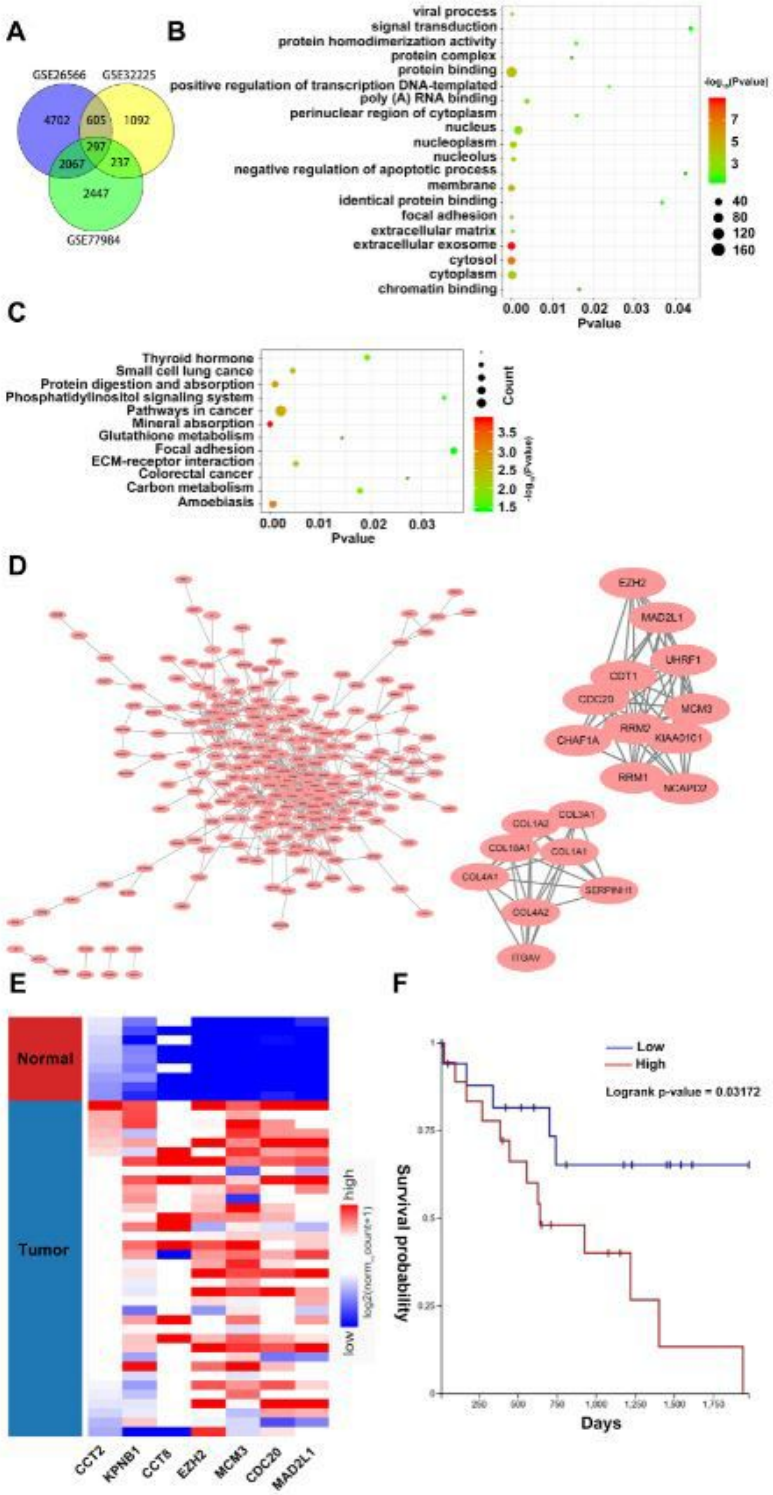

Figure 1

bioinformatic analysis found MAD2L1 expressed strength in CCA and predicted poor prognosis. (A) DEGs were selected with a log (fold change) >1 and P-value <0.01 among the mRNA expression profiling sets GSE26566, GSE32225 and GSE77984. (B) According to P-value < 0.05, the bubble chart showed the top 20 significant pathways of GO functional enrichment of the DEGs. (C) The bubble chart showed all the differential pathways of KEGG pathways enrichment of the DEGs (p < 0.05). (D) The PPI network of

DEGs was constructed using Cytoscape. The most two significant modules were obtained from the PPI network. (E) The hierarchical clustering of 7 hub genes was created using UCSC. The upregulation of genes is marked in red; downregulation of genes is marked in blue. (F) Overall survival analyzes of MAD2L1 was performed using UCSC Xena online platform. P<0.05 was considered statistically significant.

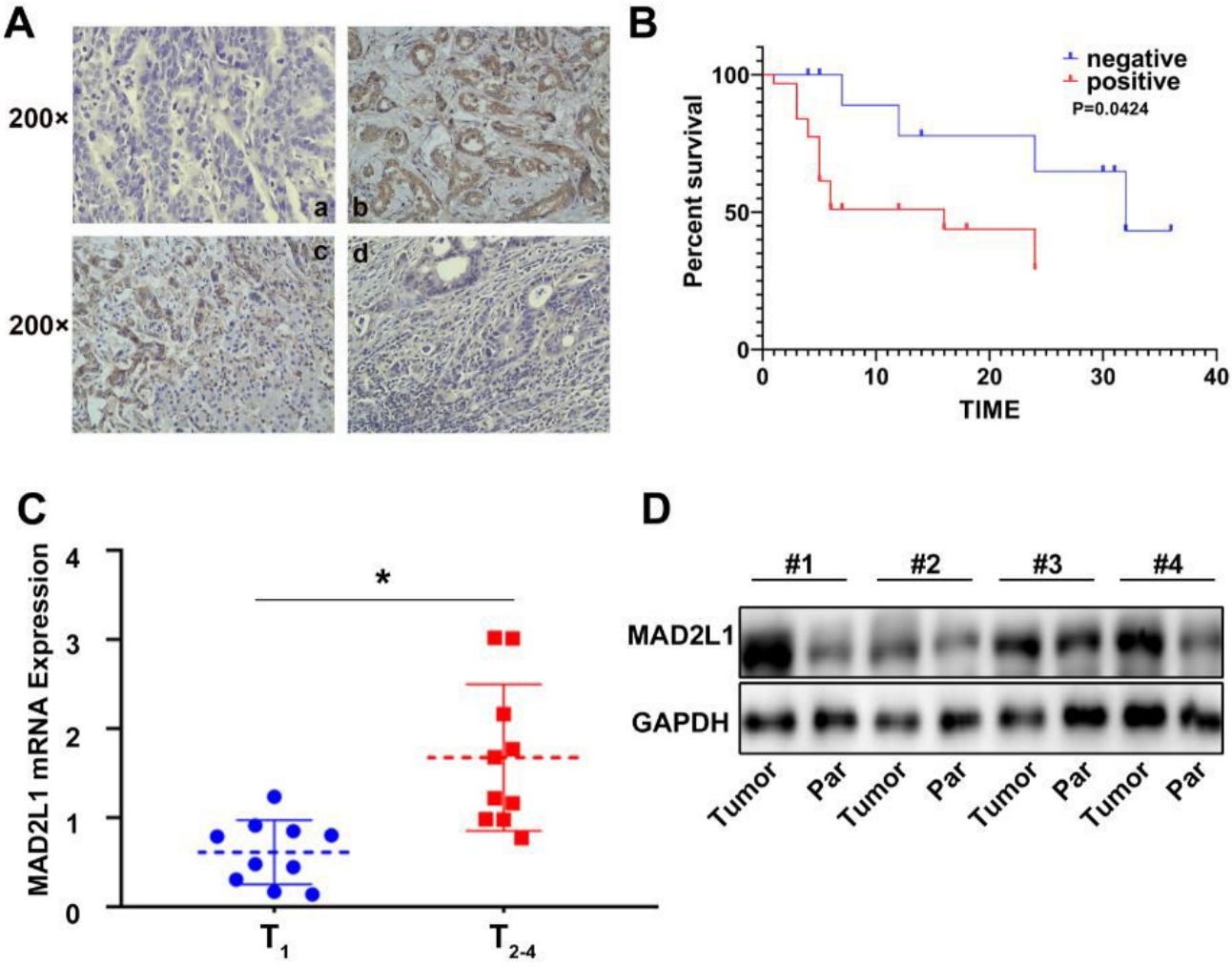

Figure 2

MAD2L1 expression and clinical outcome. (A) MAD2L1 was exclusively expressed in primary CCA, par-carcinoma, and metastatic lymph nodes by IHC (original magnifications ×200). Representative MAD2L1-negative tumor (a) and MAD2L1-positive tumor (b). MAD2L1-positive tumor surrounded by negatively stained normal tissue (c) and MAD2L1 weak-positive staining in representative lymph node metastasis (d). (B) The postoperative survival analysis of 42 patients with at least 12 months of follow-up. (C) MAD2L1 mRNA expression in 10 fresh cancer with T1 versus ten with T2-4 sizes. (D) MAD2L1 protein expression in paired tumor and adjacent tissues. P<0.05 was considered statistically significant.

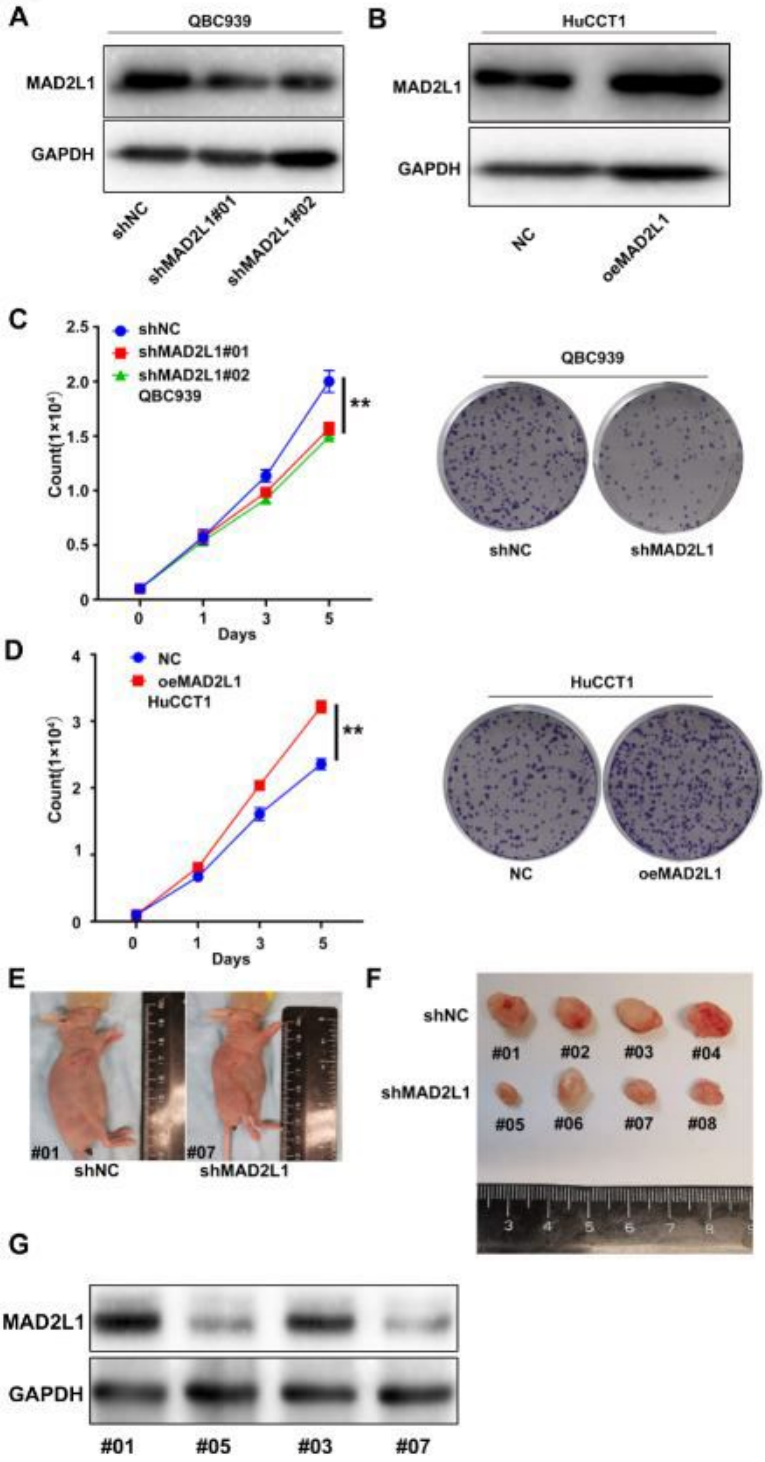

Figure 3

MAD2L1 promoted tumor progression through increasing cell growth. (A) Western blot verification of MAD2L1 knockdown in QBC939 cells. (B) Western blot verification of MAD2L1 over-expression in HuCCT1 cells. (C) Cell counting (left) and colony formation (right) were performed to assay cell growth after knocking down MAD2L1 with the shMAD2L1 (#1 and #2). (D) Cell counting (left) and colony formation (right) were performed to assay cell growth after over-expressing MAD2L1 with MAD2L1-cDNA.

(E) Representative nude mice from two groups of Vivo models. (F) Gross CCA tumor samples of nude mice after four weeks' injection of QBC939 cells. (G) MAD2L1 expression of the representative samples from two groups was detected by western blot.

Supplementary Files

This is a list of supplementary files associated with this preprint. Click to download.

- FigS1.jpg
- Table1.jpg